

Impact of Fluoride on Epigenetic and Metabolic Dynamics in the Ileum: Unveiling the Adaptive Responses in NOD Mice

Marília Afonso Rabelo Buzalaf¹, Aline Dionizio¹, Aislan Quintiliano Delgado², João Paulo Zanardini de Lara¹, Ana Carolina Magalhães¹, José Roberto Bosqueiro², Juliana Sanches Trevizol¹, and Nathalia Rabelo Buzalaf¹

¹Universidade de Sao Paulo Faculdade de Odontologia de Bauru

²Universidade Estadual Paulista Julio de Mesquita Filho - Campus de Bauru

March 15, 2024

Abstract

Fluoride (F) has been employed worldwide to control dental caries. More recently, it has been suggested that the consumption of low doses of F in the drinking water may reduce blood glucose levels, introducing a new perspective for the use of F for the management of blood glucose. However, the exact mechanism by which F affects blood glucose levels remains largely unexplored. Given that the small gut plays a pivotal role in glucose homeostasis, the aim of this present study was to investigate the proteomic changes induced by low doses of F in the ileum of female non-obese-diabetic (NOD) mice. Forty-two female NOD mice were divided into two groups based on the F concentration in their for 14 weeks: 0 (control) or 10 mg/L. At the end of the experimental period, the ileum was collected for proteomic and Western Blotting analyses. Proteomic analysis indicated an increase in isoforms of actin, gastrotropin (confirmed by Western Blotting), several H2B histones and enzymes involved in antioxidant processes, as well as a decrease in enzymes essential for energy metabolism. In summary, our data indicates an adaptive response of the organism to preserve protein synthesis in the ileum, despite significant alterations in energy metabolism typically induced by F, therefore highlighting the safety of controlled fluoridation in water supplies.

Impact of Fluoride on Epigenetic and Metabolic Dynamics in the Ileum: Unveiling the Adaptive Responses in NOD Mice

Authors:

+Juliana Sanches Trevizol¹(julianatrevizol@gmail.com)

+Nathalia Rabelo Buzalaf¹(nathaliabuzalaf@hotmail.com)

Aline Dionizio¹ (alinesdionizio@usp.br)

Aislan Quintiliano Delgado²(aislan.quintiliano@gmail.com)

João Paulo Zanardini de Lara¹(joaopaulolara95@hotmail.com)

Ana Carolina Magalhães¹ (acm@usp.br)

José Roberto Bosqueiro³ (jose.bosqueiro@unesp.br)

Marília Afonso Rabelo Buzalaf^{1*} (mbuzalaf@fob.usp.br)

¹ Department of Biological Sciences, Bauru School of Dentistry, University of São Paulo, Bauru, Brazil.

² Institute of Biosciences, São Paulo State University, Botucatu, São Paulo, Brazil.

³Department of Physical Education, Faculty of Science, São Paulo State University, Bauru, São Paulo, Brazil.

*** Corresponding author**

Marília Afonso Rabelo Buzalaf- Alameda Octávio Pinheiro Brisolla, 9-75

Bauru-SP, Brazil, 17012-901- Phone: # 55 14 3235-8346- Email: mbuzalaf@fob.usp.br

+ Juliana Sanches Trevizol and Nathalia Rabelo Buzalaf contributed equally to this work

ABSTRACT

Fluoride (F) has been employed worldwide to control dental caries. More recently, it has been suggested that the consumption of low doses of F in the drinking water may reduce blood glucose levels, introducing a new perspective for the use of F for the management of blood glucose. However, the exact mechanism by which F affects blood glucose levels remains largely unexplored. Given that the small gut plays a pivotal role in glucose homeostasis, the aim of this present study was to investigate the proteomic changes induced by low doses of F in the ileum of female non-obese-diabetic (NOD) mice. Forty-two female NOD mice were divided into two groups based on the F concentration in their for 14 weeks: 0 (control) or 10 mg/L. At the end of the experimental period, the ileum was collected for proteomic and Western Blotting analyses. Proteomic analysis indicated an increase in isoforms of actin, gastrotropin (confirmed by Western Blotting), several H2B histones and enzymes involved in antioxidant processes, as well as a decrease in enzymes essential for energy metabolism. In summary, our data indicates an adaptive response of the organism to preserve protein synthesis in the ileum, despite significant alterations in energy metabolism typically induced by F, therefore highlighting the safety of controlled fluoridation in water supplies.

Keywords: ileum, diabetes, fluoride, glucose homeostasis, epigenetic

INTRODUCTION

Fluoride (F) has been widely employed worldwide to control dental caries, primarily through drinking water and toothpaste (Bratthall et al. 1996; Buzalaf and Whitford 2011; Iheozor-Ejiofor et al. 2015). However, excessive ingestion may cause various alterations in the organism, including oxidative stress (Pereira et al. 2018; Pereira et al. 2016; Pereira et al. 2013), perturbations in the lipid metabolism (Dionizio et al. 2018a), changes in intracellular homeostasis and cell cycle, leading to apoptosis (Barbier et al. 2010), and morphological and proteomic alterations in the duodenum (Melo et al. 2017), jejunum (Dionizio et al. 2018b) and ileum (Dionizio et al. 2021).

The gastrointestinal tract (GIT) is the main route of exposure to F. Approximately 25% of the ingested F is absorbed in the stomach as hydrofluoric acid, (Whitford and Pashley 1984), and around 75% is absorbed in the small intestine in its ionic form (F⁻), independent of pH (Nopakun and Messer 1990; Nopakun et al. 1989). Consequently, gastrointestinal symptoms like nausea, vomiting, abdominal pain, and diarrhea are the first signs of F toxicity (Whitford 2011).

More recently, it has been suggested that consumption of low doses of F in drinking water, similar to those added to artificially fluoridated water, may increase insulin sensitivity or reduce blood glucose levels (Lima Leite et al. 2014; Lobo et al. 2015; Malvezzi et al. 2019; Trevizol et al. 2020; Trevizol et al. 2023), which is very relevant from the perspective of public health, since water fluoridation is recognized among the top ten public health achievements of the last century (Centers for Disease and Prevention 1999). However, the exact mechanisms by which F influences glucose homeostasis remain unclear.

The small gut is central to glucose homeostasis, as the jejunum senses nutrients and regulates hepatic glucose production, and the entire small gut secretes both glucagon-like peptide-1 (GLP-1) and glucose-dependent insulinotropic peptide (GIP), enhancing insulin secretion (Kamvissi-Lorenz et al. 2017). GLP-1 enhances insulin secretion, accounting for around 70% of the insulin secretion in the presence of high levels of glucose (Miyawaki et al. 2002).

In this study, NOD mice, a validated model for evaluating agents and protocols that prevent or reverse type 1 diabetes (T1D) (Mullen 2017), were used to assess the proteomic changes induced by low doses of F in the ileum. This aims to provide insights into the mechanisms by which F affects glucose homeostasis.

MATERIAL AND METHODS

Animals, fluoride treatment and ileum collection

The experimental protocol was approved by the Animals Ethics Committee of Bauru School of Dentistry (CEUA-Proc. 013/2017). Forty-two female NOD mice were randomly divided into two groups based on the fluoride concentration (as sodium fluoride) in the drinking water administered *ad libitum* for 14 weeks: 0 (control) or 10 mgF/L (as sodium fluoride). The drinking water was administered *ad libitum* to the animals for 14 weeks (Trevizol et al. 2020). This F concentration aims to mimic the consumption of water from the public supply by humans, since the metabolism of F by rodents is 5-10 times faster compared to humans (Dunipace et al. 1995). Female NOD mice were selected because they develop insulinitis and diabetes to a higher degree than their male counterparts. The treatment period of 14 weeks was chosen because insulinitis starts at 2-4 and 5-7 weeks in females and males, respectively, and the development of hyperglycemia is observed between 12 and 30 weeks (Mullen 2017). During the experimental period, the animals received low F (~ 2 mg/Kg) and normocaloric diet *ad libitum*. The animals were euthanized at the conclusion of the experimental period (exposure to CO₂ followed by decapitation). The ileum was collected following the procedure described in a previous publication (Dionizio et al. 2021) for proteomic and western blotting analyses (n=12 animals per group). Plasma fluoride, plasma glucose and plasma insulin were assayed and the results are reported in a previous publication (Trevizol et al. 2020).

Proteomics and bioinformatics analyses

The proteomic analysis was performed exactly as previously described (Dionizio et al., 2018). Briefly, the ileum was homogenized, proteins were extracted (lysis buffer A - 7 M urea, 2 M thiourea, 40 mM DTT, all in AMBIC solution) and the samples were quantified using the Bradford method (Bradford 1976). Samples were then reduced (5 mM DTT; BioRad, cat# 161-0611) and alkylated (10 mM IAA; GE, cat# RPN 6302V). Digestion was performed by the addition of 2% (w/w) trypsin overnight (Promega, cat #V5280). To stop the digestion, 5% TFA was added. Supernatant was purified using C 18 Spin columns (Pierce, cat #89870) and then resuspended in a solution containing 3% ACN and 0.1% formic acid.

The Xevo G2 (Waters) mass spectrometer coupled to the nanoACQUITY (Waters) system for the peptide analysis and Protein Lynx Global Server (PLGS) version 3.03 software was used to process and search for continuous LC-MSE data, as previously described (Dionizio et al. 2020; Trevizol et al. 2020). Peptides were identified using the software's ion counting algorithm and a search on the updated *Mus musculus* database (UniProtKB). The PLGS detected difference in expression between the groups, used t-test, with $p < 0,05$. The software CYTOSCAPE® (Java®) was employed to construct networks of molecular interaction between the identified proteins, supported by ClusterMarker® and ClueGO applications.

The mass spectrometry proteomics data have been deposited at the ProteomeXchange Consortium (<http://proteomecentral.proteomexchange.org>) via the PRIDE partner repository (Perez-Riverol et al. 2019) with the dataset identifier PXD031865.

Western blotting analysis

The Western blotting was conducted as previously described (Dionizio et al. 2021; Yan et al. 2012). Ileum protein extracts were obtained by lysing homogenized tissue in lysis buffer A, supplemented with protease inhibitors (Roche Diagnostics, Mannheim, Germany). Protein samples (40 μ g) were resolved in 10% Tris-HCl polyacrylamide gels and subsequently transferred to a Polyvinylidene difluoride (PVDF) membrane. Membranes were probed with commercially available *Gastrotropin* (1:500 dilution) (Abcam, Cambridge, MA, USA) and β - $\text{A}\zeta\text{TIVV}$ (1:200 dilution), followed by HRP-conjugated anti-rabbit antibody (1:10000) for *Gastrotropin* and β - $\text{A}\zeta\text{TIVV}$ (1:1000 dilution) (Cell Signaling, Danvers, MA, USA) and ECL Plus detection reagents (GE Biosciences, Piscataway, NJ, USA). The relative *Gastrotropin* and β - $\text{A}\zeta\text{TIVV}$ band densities

were determined by densitometrical analysis using the Image Studio Lite software from LI-COR Corporate Offices-US (Lincoln, Nebraska USA). In each case, density values of bands were corrected by subtraction of the background values. The results were expressed as the ratio of *Gastrotropin* to β -*Actinin*. For Western blotting data, the software GraphPad Prism (version 7.0 for Windows, La Jolla, CA, USA) was used. Data were analyzed by Kolmogorov–Smirnov test for data homogeneity and Mann-Whitney Test with $p = 0.0037$.

RESULTS

Proteomic analysis

In the proteomic analysis of the ileum, a total of 129 proteins with different expression were identified. The number of up- and down-regulated proteins identified in the 10 mgF/L group compared to the control group (0 mgF/L) was 15 and 114, respectively (Table 1). Among the up-regulated proteins, *Actins*, *Gastrotropin* and several *H2B histones* were found. Conversely, among the down-regulated proteins, were *H2A*, *H3* and *H4* histones, in addition to enzymes involved in energy metabolism, such as *Alpha-enolase*, *Malate dehydrogenase*, *Pyruvate Kinase PKM*, *Aldehyde dehydrogenase*, as well as several antioxidant enzymes, including isoforms of *Glutathione-S-Transferase* and *Peroxisredoxin* (Table 1).

Table 1. Differently expressed proteins from the ileum of 20-week-old female NOD mice, treated for 14 weeks with water containing 10 mg/L fluoride (as NaF) or not (control).

^a Access Number	Protein name	PLGS score	^b Ratio 10 mgF/L vs control
P51162	Gastrotropin	847	2.20
P70696	Histone H2B type 1-A	507	1.70
Q64524	Histone H2B type 2-E	3535	1.68
Q9D2U9	Histone H2B type 3-A	3535	1.68
Q8CGP0	Histone H2B type 3-B	3535	1.67
Q8CGP1	Histone H2B type 1-K	3856	1.58
Q64525	Histone H2B type 2-B	3856	1.58
Q64475	Histone H2B type 1-B	3856	1.57
P10853	Histone H2B type 1-F/J/L	3856	1.57
P10854	Histone H2B type 1-M	3856	1.57
Q8CGP2	Histone H2B type 1-P	3856	1.57
Q6ZWY9	Histone H2B type 1-C/E/G	3856	1.55
Q64478	Histone H2B type 1-H	3856	1.55
P63260	Actin_ cytoplasmic 2	5000	1.15
P60710	Actin_ cytoplasmic 1	5000	1.14
P68134	Actin_ alpha skeletal muscle	4953	0.83
Q9CWF2	Tubulin beta-2B chain	365	0.82
P68372	Tubulin beta-4B chain	316	0.82
Q7TMM9	Tubulin beta-2A chain	365	0.81
P99024	Tubulin beta-5 chain	365	0.81
P01942	Hemoglobin subunit alpha	633	0.80
P07724	Albumin	723	0.80
Q9D6F9	Tubulin beta-4A chain	243	0.79
Q60605	Myosin light polypeptide 6	1816	0.79
P35700	Peroxisredoxin-1	264	0.76

^a Access Number	Protein name	PLGS score	^b Ratio 10 mgF/L vs control
Q03265	ATP synthase subunit alpha_ mitochondrial	237	0.75
P63268	Actin_ gamma-enteric smooth muscle	6388	0.73
P31001	Desmin	215	0.73
P63101	14-3-3 protein zeta/delta	257	0.72
P11499	Heat shock protein HSP 90-beta	1693	0.72
P06151	L-lactate dehydrogenase A chain	115	0.71
Q8K419	Galectin-4	96	0.70
P68368	Tubulin alpha-4A chain	276	0.70
P00405	Cytochrome c oxidase subunit 2	163	0.70
P18760	Cofilin-1	301	0.70
Q9JJZ2	Tubulin alpha-8 chain	137	0.70
P08249	Malate dehydrogenase_- mitochondrial	210	0.69
Q9CZS1	Aldehyde dehydrogenase X_ mitochondrial	261	0.68
Q9CQ19	Myosin regulatory light polypeptide 9	1263	0.68
O08638	Myosin-11	629	0.68
P17182	Alpha-enolase	178	0.68
P68373	Tubulin alpha-1C chain	229	0.68
Q3THE2	Myosin regulatory light chain 12B	946	0.67
P68369	Tubulin alpha-1A chain	281	0.67
P68033	Actin_ alpha cardiac muscle 1	6497	0.66
Q64433	10 kDa heat shock protein_ mitochondrial	233	0.66
Q6URW6	Myosin-14	97	0.65
P62962	Profilin-1	364	0.65
P05213	Tubulin alpha-1B chain	317	0.65
Q8CGP5	Histone H2A type 1-F	9599	0.64
P05214	Tubulin alpha-3 chain	240	0.64
P08113	Endoplasmic reticulum chaperone	760	0.64
Q8VDD5	Myosin-9	163	0.63
P62737	Actin_ aortic smooth muscle	6479	0.63
Q8K0C5	Zymogen granule membrane protein 16	1227	0.62
Q8CI43	Myosin light chain 6B	94	0.61
Q8R1M2	Histone H2A.J	9599	0.61

^a Access Number	Protein name	PLGS score	^b Ratio 10 mgF/L vs control
P17742	Peptidyl-prolyl cis-trans isomerase A	116	0.61
Q9R100	Cadherin-17	489	0.58
C0HKE5	Histone H2A type 1-G	9599	0.58
C0HKE8	Histone H2A type 1-O	9599	0.58
P62806	Histone H4	3749	0.58
Q9EPB4	Apoptosis-associated speck-like protein containing a CARD	687	0.57
Q8BG05	Heterogeneous nuclear ribonucleoprotein A3	306	0.57
C0HKE2	Histone H2A type 1-C	9599	0.57
Q6GSS7	Histone H2A type 2-A	9599	0.57
Q9D1A2	Cytosolic non-specific dipeptidase	1074	0.56
Q64523	Histone H2A type 2-C	9599	0.56
Q8BFU2	Histone H2A type 3	9599	0.56
P58252	Elongation factor 2	690	0.55
C0HKE3	Histone H2A type 1-D	9599	0.55
C0HKE7	Histone H2A type 1-N	9599	0.55
P52480	Pyruvate kinase PKM	89	0.55
Q8QZR3	Pyrethroid hydrolase Ces2a	773	0.55
C0HKE6	Histone H2A type 1-I	9599	0.55
Q61879	Myosin-10	79	0.54
C0HKE9	Histone H2A type 1-P	9599	0.54
O88569	Heterogeneous nuclear ribonucleoproteins A2/B1	206	0.53
Q6P8J7	Creatine kinase S-type_ mitochondrial	50	0.53
C0HKE1	Histone H2A type 1-B	9599	0.53
P14152	Malate dehydrogenase_- cytoplasmic	130	0.53
Q04447	Creatine kinase B-type	95	0.53
Q8CGP6	Histone H2A type 1-H	9599	0.53
Q61696	Heat shock 70 kDa protein 1A	83	0.52
Q8CGP7	Histone H2A type 1-K	9599	0.52
P00329	Alcohol dehydrogenase 1	1018	0.51
P29758	Ornithine aminotransferase_- mitochondrial	81	0.51
P17879	Heat shock 70 kDa protein 1B	83	0.50
C0HKE4	Histone H2A type 1-E	9599	0.50

^a Access Number	Protein name	PLGS score	^b Ratio 10 mgF/L vs control
P68040	Receptor of activated protein C kinase 1	713	0.49
Q6PIE5	Sodium/potassium-transporting ATPase subunit alpha-2	45	0.48
P10630	Eukaryotic initiation factor 4A-II	492	0.48
P16125	L-lactate dehydrogenase B chain	30	0.47
Q3THW5	Histone H2A.V	515	0.47
P37804	Transgelin	531	0.47
P24549	Retinal dehydrogenase 1	538	0.46
P84228	Histone H3.2	309	0.46
P02301	Histone H3.3C	309	0.46
Q9R0P5	Dextrin	565	0.46
P27661	Histone H2AX	515	0.46
Q9D312	Keratin_ type I cytoskeletal 20	857	0.46
Q6PIC6	Sodium/potassium-transporting ATPase subunit alpha-3	45	0.45
P63038	60 kDa heat shock protein_-mitochondrial	515	0.44
P68433	Histone H3.1	309	0.44
P0C0S6	Histone H2A.Z	515	0.44
Q64522	Histone H2A type 2-B	457	0.44
P14094	Sodium/potassium-transporting ATPase subunit beta-1	1012	0.44
P84244	Histone H3.3	309	0.44
Q8C196	Carbamoyl-phosphate synthase [ammonia]_-mitochondrial	391	0.44
P46425	Glutathione S-transferase P 2	1244	0.44
P00342	L-lactate dehydrogenase C chain	30	0.43
P60843	Eukaryotic initiation factor 4A-I	612	0.43

^a Access Number	Protein name	PLGS score	^b Ratio 10 mgF/L vs control
P19157	Glutathione S-transferase P 1	1454	0.42
P23492	Purine nucleoside phosphorylase	739	0.41
Q8BK48	Pyrethroid hydrolase Ces2e	1503	0.41
P38647	Stress-70 protein_-mitochondrial	371	0.41
Q9JLJ2	4-trimethylaminobutyraldehyde dehydrogenase	151	0.40
P55050	Fatty acid-binding protein_ intestinal	1588	0.37
Q9CZU6	Citrate synthase_-mitochondrial	906	0.36
Q8BWT1	3-ketoacyl-CoA thiolase_-mitochondrial	335	0.36
O08601	Microsomal triglyceride transfer protein large subunit	938	0.36
Q8VDN2	Sodium/potassium-transporting ATPase subunit alpha-1	80	0.36
O08709	Peroxiredoxin-6	1498	0.36
P30275	Creatine kinase U-type_ mitochondrial	106	0.34
Q9CZ13	Cytochrome b-c1 complex subunit 1_ mitochondrial	289	0.34
P31786	Acyl-CoA-binding protein	2152	0.33
Q3V0K9	Plastin-1	844	0.32
Q9CPY7	Cytosol aminopeptidase	184	0.30
Q08652	Retinol-binding protein 2	773	0.16

^a Identification is based on the protein ID obtained from the UniProt database; only reviewed proteins (<http://www.uniprot.org/>).

^b Proteins with significantly altered expression are arranged according to ratio.

Proteins and bolds have a ratio [?] 2

The biological processes most affected by F treatment in terms of functional classification were Chromatin Remodeling (20%), Cytoskeleton Structural Constituent (16%), Actin filament-based movements (11%), Peroxidase activity (6 %) and Retinoid metabolic process (6%) (Figure 1).

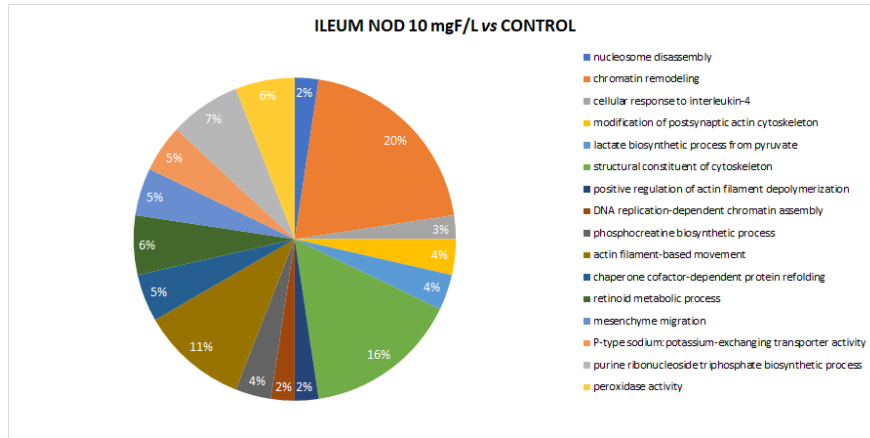


Figure 1 . Functional distribution of proteins identified with differential expression in the ileum of NOD female mice treated with water containing 10 mgF/L or 0 mgF/L (control). Protein categories are based on Gene Ontology (GO) “Biological Process” annotation. Significance of terms (Kappa=0.04) and distribution according to the percentage of the number of genes. The protein accession number was provided by UniProt. GO was evaluated according to ClueGo plugin and Cytoscape 3.7.2 software

In the network generated by ClusterMarker2, when comparing the expression of altered proteins in the treated group (10 mgF/L) in relation to the control group (0 mgF/L), it was possible to observe many proteins interacting with *High mobility group protein HMGI-C* (P52927), *Actin cytoplasmic 2* (P63260), *Actin alpha skeletal muscle* (P68134) and *Microsomal triglyceride transfer protein large subunit* (O08601) (Figure 2).

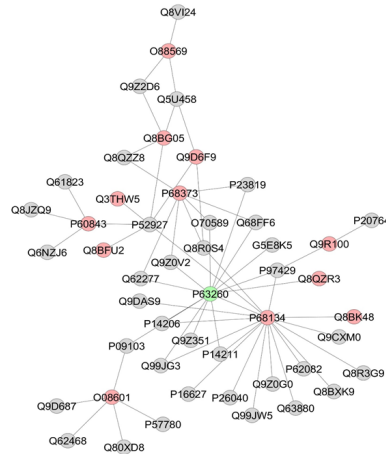


Figure 2. Ileum subnetwork generated by ClusterMarker for comparison 10 mgF/L vs. 10 mgF/L. Control (0 mgF/L). The color of the node indicates the differential expression of the protein with its access code obtained from the UniProt protein database (<http://uniprot.org/>). Light green and light red nodes indicate upregulated and downregulated proteins, respectively, in the 10 mgF/L group, compared to the control group. The gray nodes represent interacting proteins that are offered by Cytoscape, but that were not identified in the present study.

Western Blotting

Western blotting confirmed that *Gastrotropin* was significantly increased upon exposure F, as revealed by proteomic analysis (Figure 3).

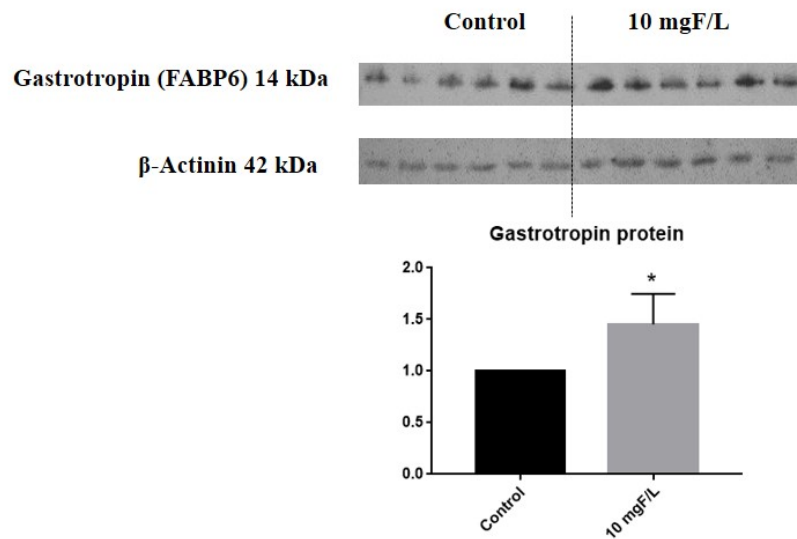


Figure 3- Representative expression of proteins *Gastrotropin* and constitutive β -Actinin in samples of individual animals ($n = 6$) from each group. Densitometric analysis was performed for 6 animals per group. Densitometry was analyzed using the software Image Studio Lite. Bars indicate SD. $n = 6$

DISCUSSION

The results of plasma F concentration, glucose and plasma insulin are reported in a previous publication (Trevizol et al. 2020). Low-dose F exposure significantly elevated plasma F levels, lowered blood glucose by 20%, and did not impact insulinemia. These data are extremely relevant from a public health point of view, since water fluoridation, a worldwide recognized measure for the prevention of dental caries (Buzalaf 2018), could also aid in controlling hyperglycemia. However, the potential mechanisms underlying the effects of F on glycemic are yet to be elucidated. A feasible explanation could be the well-documented effects of F in diminishing energy metabolism (Araujo et al. 2019; Dionizio et al. 2021; Dionizio et al. 2018b; Khan et al. 2018; Malvezzi et al. 2019; Trevizol et al. 2020; Trevizol et al. 2023). Exposure to F has been linked to changes in enzymes involved in energy metabolism and the antioxidant system, as observed in the liver of NOD mice (Malvezzi et al. 2019; Trevizol et al. 2020) and various intestinal segments of rats (Dionizio et al. 2021; Dionizio et al. 2018b; Melo et al. 2017).

In the current study, we generally noted a reduction in several enzymes involved in energy metabolism, such as *Alpha-enolase*, *Malate dehydrogenase*, *Pyruvate Kinase PKM*, *Aldehyde dehydrogenase*, observed both in the duodenum (unpublished data) and in the ileum of F-treated mice. A decrease in glycolytic enzymes following exposure to low doses of F has been similarly documented in other studies with rats (Araujo et al. 2019) and NOD mice (Malvezzi et al. 2019; Trevizol et al. 2020). Additionally, there was also a reduction in proteins related to lipid metabolism, such as *Fatty acid-binding* proteins, which play a role in intracellular lipid transport (Consortium 2023). Among these proteins is *Gastrotropin*, also known as *Fatty acid-binding protein 6*, an important transport protein involved in the enterohepatic circulation of bile salts. Predominantly expressed in the ileum, it participates in the absorption of vitamin B12 and binds to bile acids, crucial for the effective digestion and absorption of dietary fats (Davis and Attie 2008; Grober et al. 1999; Iizumi et al. 2007; Landrier et al. 2006; Marvin-Guy et al. 2005; Thompson et al. 2017).

In this study, *Gastrotropin* levels increased in the ileum of NOD mice after F treatment, contrasting with findings in the ileum of rats treated with a similar concentration of F in the drinking water, where this protein was reduced (Dionizio et al. 2021). However, in the study by Dionizio et al. (2021), the mice were not diabetic, which might explain the different expression patterns observed. Modifications in receptors and proteins related to bile acids (BAs) may be crucial in regulating BAs, lipids, and glucose homeostasis, as well as managing inflammatory responses, barrier function, and preventing bacterial translocation in the intestinal tract (Ding et al. 2015; Gillard et al. 2022). Furthermore, other FABP family proteins such as FABP1 and FABP2, are often associated with type 2 diabetes pathology, where alterations can lead to changes in lipid metabolism and disruptions in proteins related to fatty acids, lipid transport and intestinal absorption (Sianipar et al. 2022; Tsai et al. 2020).

It is recognized that genes involved in antioxidant defense are less expressed in spontaneously diabetic lymphopenic rats (BB rats), a factor implicated in β -cell damage and the development of diabetes in these animals (Bogdani et al. 2013). In our study, we noted a reduction in peroxiredoxin and isoforms of *Glutathione S-transferase* in the ileum. In the liver of NOD mice treated with low doses of F, these enzymes were also diminished (Malvezzi et al. 2019; Trevizol et al. 2020). The observed increase in these antioxidant enzymes in the current study indicated a potential counterregulatory mechanism of detoxification in the ileum of NOD mice.

Environmental factors can cause epigenetic changes that regulate gene expression and influence immune cell function. Epigenetics provides multiple molecular mechanisms to elucidate the environmental effects implicated in the development of autoimmune diabetes. The three primary epigenetic modifications are DNA methylation, histone modification, and microRNA alteration (Xie et al. 2014). In the ileum, we noted significant changes in histone expression, histone-modifying proteins, and numerous other proteins involved in transcription and translation, such as ribonucleoproteins. This epigenetic influence of F on histone modification was similarly observed in the islets of female NOD mice (Trevizol et al. 2023). Additionally, dysregulation in histone acetylation, governed by histone deacetylases (HDACs) and histone acetyltransferases (HATs), is implicated in diabetes pathogenesis (Gray and De Meyts 2005). Histone acetylation has been demonstrated to preserve insulin secretion under cytokine insult and prevent NF- κ B-induced apoptosis in β -cell lines and islets from newborn mice (Larsen et al. 2007). In our previous study (Trevizol et al. 2023), we observed an increase in inflammatory infiltrate in the group exposed to 10 mgF/L in their drinking water. Additionally, proteomic analysis of the islets revealed substantial increases in histones H3.1 and H3.2 (about 100-fold), as well as in histone H4 (more than 60-fold), alongside a 6-fold rise in histone acetyltransferase KAT6B and histone acetyltransferase KAT8, exclusively found with F treatment. The proportion of histone H3 acetylation was also assessed, showing more than a 2-fold increase in the F-exposed group compared to the control, though the difference was not significant. The acetylation of H3K14 was analyzed as it is a target of KAT6B and KAT8.

During histone acetylation, an acetyl functional group is transferred from acetyl Co-A to the histone (Gruber et al. 2019). In the current study, Krebs' cycle enzymes, like malate dehydrogenase and citrate synthase, were diminished in the ileum. These observations suggest a decrease in Krebs' cycle flow, potentially reducing acetyl Co-A levels. Furthermore, the reduction of enzymes in the glycolytic pathway, also noted in our findings, contributes to the lowered acetyl Co-A levels (Wellen et al. 2009). Therefore, the substantial alterations in the expression of histones, histone-modifying proteins and various proteins involved in transcription and translation may represent effort to sustain translation amidst reduced acetyl Co-A availability.

We consider these findings particularly intriguing, as recent research has shown F-induced hypermethylation in crucial genes linked to various toxicity effects (Ma et al. 2020; Meng et al. 2021). Indeed, the concept of F-induced epigenetic changes has only recently emerged in scientific literature and warrants further investigation. In summary, our data indicate an adaptive response of the organism to preserve protein synthesis in the ileum, despite significant alterations in energy metabolism typically induced by F, therefore highlighting the safety of controlled fluoridation in water supplies.

Significance Statement

The consumption of low doses of fluoride in the drinking water may increase insulin sensitivity or reduce blood glucose levels. However, the exact mechanisms by which fluoride influences glucose homeostasis remain unclear. Considering that the small gut is central to glucose homeostasis, here we investigated the proteomic changes induced by low doses of fluoride (similar to those added to the drinking water) in the ileum of non-obese-diabetic mice. We found an increase in gastrotropin, histones and antioxidant enzymes, and decrease in enzymes involved in energy metabolism. These results indicate an adaptive response of the organism to preserve protein synthesis in the ileum, despite significant alterations in energy metabolism, therefore highlighting the safety of controlled fluoridation of water supplies.

Declarations

The study was approved by the Animals Ethics Committee of Bauru School of Dentistry, University of São Paulo (CEUA-Proc. 013/2017).

Author's contributions

J.S.T, A.D, M.B and J.R.B conceived the experiments. J.S.T, A.D, A.Q.D, A.C.M, M.B and J.R.B conducted the experiments. J.S.T, A.D, A.Q.D, T.M.C, J.R.B, T.M.O.V and N.R.B participated in the research experiments. J.S.T, A.Q.D, T.M.C, C.F.S.R, J.R.B, M.B and N.R.B participated in the analyses. J.S.T, N.R.B, A.C.M. and M.B. drafted the article, analyzed and interpreted the results. All authors revised and approved the manuscript.

Conflict of interest statement: The authors declare no conflict of interest.

Data Availability Statement: All the data that are presented are included in the article materials and further inquiries can be directed to the corresponding author.

Acknowledgements: The authors thank FAPESP (Proc. 2018/00352-8) for the concession of a scholarship to the second author.

REFERENCES

- Araujo TT, Barbosa Silva Pereira HA, Dionizio A, Sanchez CDC, de Souza Carvalho T, da Silva Fernandes M, Rabelo Buzalaf MA. 2019. Changes in energy metabolism induced by fluoride: Insights from inside the mitochondria. *Chemosphere*. 236:124357.
- Barbier O, Arreola-Mendoza L, Del Razo LM. 2010. Molecular mechanisms of fluoride toxicity. *Chem Biol Interact*. 188(2):319-333.
- Bogdani M, Henschel AM, Kansra S, Fuller JM, Geoffrey R, Jia S, Kaldunski ML, Pavletich S, Prosser S, Chen YG et al. 2013. Biobreeding rat islets exhibit reduced antioxidative defense and n-acetyl cysteine treatment delays type 1 diabetes. *J Endocrinol*. 216(2):111-123.
- Bradford MM. 1976. A rapid and sensitive method for the quantitation of microgram quantities of protein utilizing the principle of protein-dye binding. *Anal Biochem*. 72:248-254.
- Bratthall D, Hansel-Petersson G, Sundberg H. 1996. Reasons for the caries decline: What do the experts believe? *European journal of oral sciences*. 104(4 (Pt 2)):416-422; discussion 423-415, 430-412.
- Buzalaf MAR. 2018. Review of fluoride intake and appropriateness of current guidelines. *Adv Dent Res*. 29(2):157-166.
- Buzalaf MAR, Whitford GM. 2011. Fluoride metabolism. *Monographs in oral science*. 22:20-36.
- Centers for Disease C, Prevention. 1999. Ten great public health achievements—united states, 1900-1999. *MMWR Morbidity and mortality weekly report*. 48(12):241-243.
- Consortium TU. 2023. Uniprot: The universal protein knowledgebase. *Nucleic Acids Res* 51:D523–D531.

- Davis RA, Attie AD. 2008. Deletion of the ileal basolateral bile acid transporter identifies the cellular sentinels that regulate the bile acid pool. *Proceedings of the National Academy of Sciences of the United States of America*. 105(13):4965-4966.
- Ding L, Yang L, Wang Z, Huang W. 2015. Bile acid nuclear receptor fxr and digestive system diseases. *Acta pharmaceutica Sinica B*. 5(2):135-144.
- Dionizio A, Pereira H, Araujo TT, Sabino-Arias IT, Fernandes MS, Oliveira KA, Raymundo FS, Cestari TM, Nogueira FN, Carvalho RA et al. 2018a. Effect of duration of exposure to fluoride and type of diet on lipid parameters and de novo lipogenesis. *Biological trace element research*. 190(1):157-171.
- Dionizio A, Uyghurturk DA, Melo CGS, Sabino-Arias IT, Araujo TT, Ventura TMS, Perles J, Zanoni JN, Den Besten P, Buzalaf MAR. 2021. Intestinal changes associated with fluoride exposure in rats: Integrative morphological, proteomic and microbiome analyses. *Chemosphere*. 273:129607.
- Dionizio AS, Melo CGS, Sabino-Arias IT, Ventura TMS, Leite AL, Souza SRG, Santos EX, Heubel AD, Souza JG, Perles J et al. 2018b. Chronic treatment with fluoride affects the jejunum: Insights from proteomics and enteric innervation analysis. *Scientific reports*. 8(1):3180.
- Dionizio AS, Melo CGS, Sabino-Arias IT, Ventura TMS, Leite AL, Souza SRG, Santos EX, Heubel AD, Souza JG, Perles J et al. 2020. Effects of acute fluoride exposure on the jejunum and ileum of rats. *Science of the total environment*. 1.
- Dunipace AJ, Brizendine EJ, Zhang W, Wilson ME, Miller LL, Katz BP, Warrick JM, Stookey GK. 1995. Effect of aging on animal response to chronic fluoride exposure. *Journal of dental research*. 74(1):358-368.
- Gillard J, Clerbaux LA, Nachit M, Sempoux C, Staels B, Bindels LB, Tailleux A, Leclercq IA. 2022. Bile acids contribute to the development of non-alcoholic steatohepatitis in mice. *JHEP reports : innovation in hepatology*. 4(1):100387.
- Gray ST, De Meyts P. 2005. Role of histone and transcription factor acetylation in diabetes pathogenesis. *Diabetes-Metab Res*. 21(5):416-433.
- Grober J, Zaghini I, Fujii H, Jones SA, Kliewer SA, Willson TM, Ono T, Besnard P. 1999. Identification of a bile acid-responsive element in the human ileal bile acid-binding protein gene. Involvement of the farnesoid x receptor/9-cis-retinoic acid receptor heterodimer. *The Journal of biological chemistry*. 274(42):29749-29754.
- Gruber JJ, Geller B, Lipchik AM, Chen J, Salahudeen AA, Ram AN, Ford JM, Kuo CJ, Snyder MP. 2019. Hat1 coordinates histone production and acetylation via h4 promoter binding. *Mol Cell*. 75(4):711-724 e715.
- Iheozor-Ejiofor Z, Worthington HV, Walsh T, O'Malley L, Clarkson JE, Macey R, Alam R, Tugwell P, Welch V, Glenny AM. 2015. Water fluoridation for the prevention of dental caries. *The Cochrane database of systematic reviews*. (6):CD010856.
- Iizumi G, Sadoya Y, Hino S, Shibuya N, Kawabata H. 2007. Proteomic characterization of the site-dependent functional difference in the rat small intestine. *Biochimica et biophysica acta*. 1774(10):1289-1298.
- Kamvissi-Lorenz V, Raffaelli M, Bornstein S, Mingrone G. 2017. Role of the gut on glucose homeostasis: Lesson learned from metabolic surgery. *Curr Atheroscler Rep*. 19(2):9.
- Khan ZN, Sabino IT, de Souza Melo CG, Martini T, da Silva Pereira HAB, Buzalaf MAR. 2018. Liver proteome of mice with distinct genetic susceptibilities to fluorosis treated with different concentrations of f in the drinking water. *Biological trace element research*.
- Landrier JF, Eloranta JJ, Vavricka SR, Kullak-Ublick GA. 2006. The nuclear receptor for bile acids, fxr, transactivates human organic solute transporter-alpha and -beta genes. *American journal of physiology Gastrointestinal and liver physiology*. 290(3):G476-485.

- Larsen L, Tonnesen M, Ronn SG, Storling J, Jorgensen S, Mascagni P, Dinarello CA, Billestrup N, Mandrup-Poulsen T. 2007. Inhibition of histone deacetylases prevents cytokine-induced toxicity in beta cells. *Diabetologia*. 50(4):779-789.
- Lima Leite A, Gualium Vaz Madureira Lobo J, Barbosa da Silva Pereira HA, Silva Fernandes M, Martini T, Zucki F, Sumida DH, Rigalli A, Buzalaf MA. 2014. Proteomic analysis of gastrocnemius muscle in rats with streptozotocin-induced diabetes and chronically exposed to fluoride. *PLoS One*. 9(9):e106646.
- Lobo JG, Leite AL, Pereira HA, Fernandes MS, Peres-Buzalaf C, Sumida DH, Rigalli A, Buzalaf MA. 2015. Low-level fluoride exposure increases insulin sensitivity in experimental diabetes. *J Dent Res*. 94(7):990-997.
- Ma Y, Yao Y, Zhong N, Angwa LM, Pei J. 2020. The dose-time effects of fluoride on the expression and DNA methylation level of the promoter region of *bmp-2* and *bmp-7* in rats. *Environ Toxicol Pharmacol*. 75:103331.
- Malvezzi M, Pereira H, Dionizio A, Araujo TT, Buzalaf NR, Sabino-Arias IT, Fernandes MS, Grizzo LT, Magalhaes AC, Buzalaf MAR. 2019. Low-level fluoride exposure reduces glycemia in nod mice. *Ecotoxicology and environmental safety*. 168:198-204.
- Marvin-Guy L, Lopes LV, Affolter M, Courtet-Compondu MC, Wagniere S, Bergonzelli GE, Fay LB, Kussmann M. 2005. Proteomics of the rat gut: Analysis of the myenteric plexus-longitudinal muscle preparation. *Proteomics*. 5(10):2561-2569.
- Melo CGS, Perles J, Zanoni JN, Souza SRG, Santos EX, Leite AL, Heubel AD, CO ES, Souza JG, Buzalaf MAR. 2017. Enteric innervation combined with proteomics for the evaluation of the effects of chronic fluoride exposure on the duodenum of rats. *Scientific reports*. 7(1):1070.
- Meng X, Yao Y, Ma Y, Zhong N, Alphonse S, Pei J. 2021. Effect of fluoride in drinking water on the level of 5-methylcytosine in human and rat blood. *Environ Toxicol Pharmacol*. 81:103511.
- Miyawaki K, Yamada Y, Ban N, Ihara Y, Tsukiyama K, Zhou H, Fujimoto S, Oku A, Tsuda K, Toyokuni S et al. 2002. Inhibition of gastric inhibitory polypeptide signaling prevents obesity. *Nat Med*. 8(7):738-742.
- Mullen Y. 2017. Development of the nonobese diabetic mouse and contribution of animal models for understanding type 1 diabetes. *Pancreas*. 46(4):455-466.
- Nopakun J, Messer HH. 1990. Mechanism of fluoride absorption from the rat small-intestine. *Nutr Res*. 10(7):771-779.
- Nopakun J, Messer HH, Voller V. 1989. Fluoride absorption from the gastrointestinal tract of rats. *J Nutr*. 119(10):1411-1417.
- Pereira H, Dionizio AS, Araujo TT, Fernandes MDS, Iano FG, Buzalaf MAR. 2018. Proposed mechanism for understanding the dose- and time-dependency of the effects of fluoride in the liver. *Toxicology and applied pharmacology*. 358:68-75.
- Pereira HA, Dionizio AS, Fernandes MS, Araujo TT, Cestari TM, Buzalaf CP, Iano FG, Buzalaf MA. 2016. Fluoride intensifies hypercaloric diet-induced oxidative stress and alters lipid metabolism. *PLoS One*. 11(6):e0158121.
- Pereira HA, Leite Ade L, Charone S, Lobo JG, Cestari TM, Peres-Buzalaf C, Buzalaf MA. 2013. Proteomic analysis of liver in rats chronically exposed to fluoride. *PLoS One*. 8(9):e75343.
- Perez-Riverol Y, Csordas A, Bai J, Bernal-Llinares M, Hewapathirana S, Kundu DJ, Inuganti A, Griss J, Mayer G, Eisenacher M et al. 2019. The proteome database and related tools and resources in 2019: Improving support for quantification data. *Nucleic Acids Res*. 47(D1):D442-D450.
- Sianipar IR, Sestramita S, Pradnjaparamita T, Yumir E, Harbuwono DS, Soewondo P, Tahapary DL. 2022.

The role of intestinal-fatty acid binding proteins and chitinase-3-like protein 1 across the spectrum of dysglycemia. *Diabetes & metabolic syndrome*. 16(1):102366.

Thompson CA, Wojta K, Pulakanti K, Rao S, Dawson P, Battle MA. 2017. Gata4 is sufficient to establish jejunal versus ileal identity in the small intestine. *Cellular and molecular gastroenterology and hepatology*. 3(3):422-446.

Trevizol JS, Buzalaf NR, Dionizio A, Delgado AQ, Cestari TM, Bosqueiro JR, Magalhaes AC, Buzalaf MAR. 2020. Effects of low-level fluoride exposure on glucose homeostasis in female nod mice. *Chemosphere*. 254:126602.

Trevizol JS, Dionizio A, Delgado AQ, Ventura TMO, Ribeiro C, Ribeiro L, Buzalaf NR, Cestari TM, Magalhaes AC, Suzuki M et al. 2023. Metabolic effect of low fluoride levels in the islets of nod mice: Integrative morphological, immunohistochemical, and proteomic analyses. *Journal of applied oral science : revista FOB*. 31:e20230036.

Tsai IT, Wu CC, Hung WC, Lee TL, Hsuan CF, Wei CT, Lu YC, Yu TH, Chung FM, Lee YJ et al. 2020. Fabp1 and fabp2 as markers of diabetic nephropathy. *International journal of medical sciences*. 17(15):2338-2345.

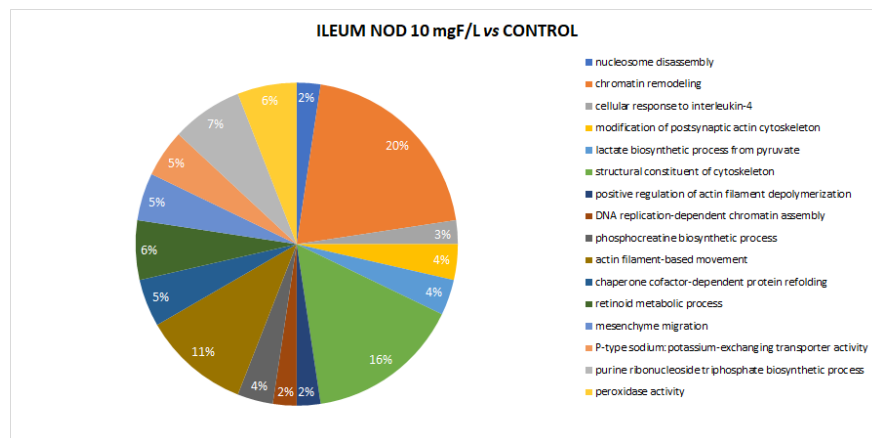
Wellen KE, Hatzivassiliou G, Sachdeva UM, Bui TV, Cross JR, Thompson CB. 2009. Atp-citrate lyase links cellular metabolism to histone acetylation. *Science*. 324(5930):1076-1080.

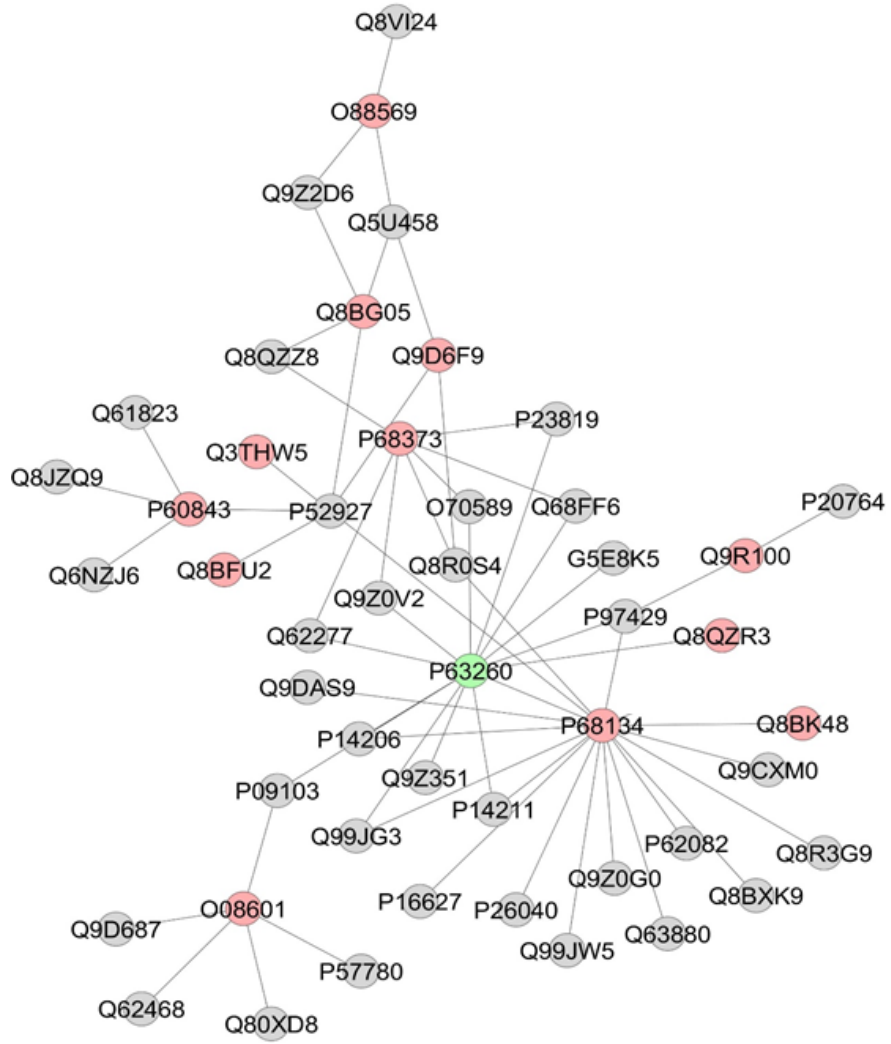
Whitford GM. 2011. Acute toxicity of ingested fluoride. *Monographs in oral science*. 22:66-80.

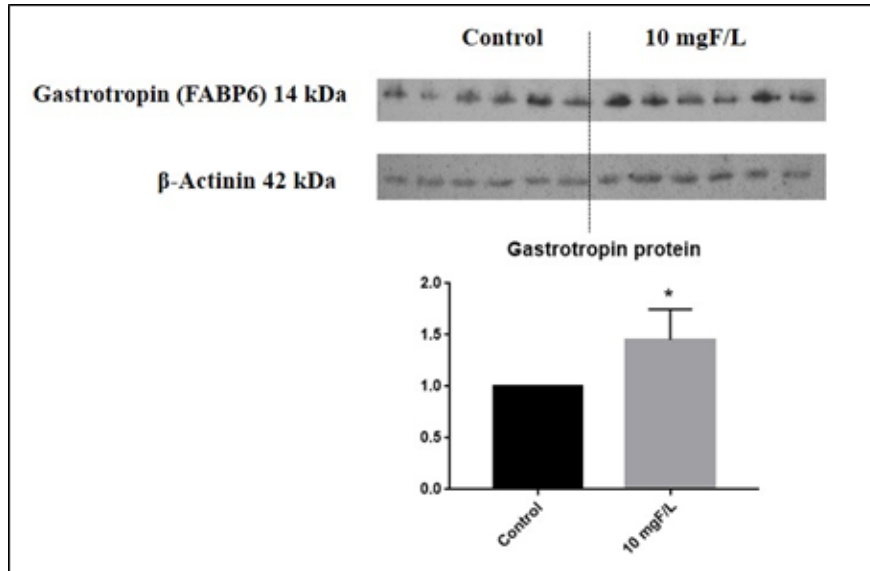
Whitford GM, Pashley DH. 1984. Fluoride absorption: The influence of gastric acidity. *Calcif Tissue Int*. 36(3):302-307.

Xie Z, Chang C, Zhou Z. 2014. Molecular mechanisms in autoimmune type 1 diabetes: A critical review. *Clin Rev Allergy Immunol*. 47(2):174-192.

Yan YX, Gong YW, Guo Y, Lv Q, Guo C, Zhuang Y, Zhang Y, Li R, Zhang XZ. 2012. Mechanical strain regulates osteoblast proliferation through integrin-mediated erk activation. *PLoS One*. 7(4):e35709.







Hosted file

Table 1.docx available at <https://authorea.com/users/755646/articles/725960-impact-of-fluoride-on-epigenetic-and-metabolic-dynamics-in-the-ileum-unveiling-the-adaptive-responses-in-nod-mice>